Ion Beam-Induced Amorphization: A Crystal-to-Glass Transition?

Harry Bernas*

CSNSM/CNRS, Université Paris-11
91405 Orsay, France

Abstract

Many static and dynamic properties of amorphous materials are universal, e.g., identical for organic or metallic glasses. This is also true for the liquid-to-glass transformation. This universality is still an open problem. Ion beams bring a novel facet to it, since they may induce the energetically unfavourable crystal-to-glass transformation. We enumerate and discuss the corresponding features in ion beam amorphization, notably those through which the beam-induced crystal-to-glass transformation resembles the Cohen–Grest liquid-to-glass percolation transition, and propose a phase diagram that relates the liquid-to-glass and crystal-to-glass transitions via recent theories of "dynamic jamming". The crystal-to-glass transition's stochastic properties suggest a study of the ion beam-solid interaction's effect on an evolving glass's ergodicity.

Contents

* E-mail: bernas@csnsm.in2p3.fr

1. Introduction

Notwithstanding their considerable differences in electronic properties, a vast compendium of organic or inorganic, insulating, semiconducting or metallic systems display remarkably similar dynamic behaviours when forced into the amorphous ("glassy") state. This has been repeatedly stressed and discussed in excellent reviews and textbooks (e.g., Anderson, 1979; Joffrin, 1979; Zallen, 1983; Jäckle, 1986; Cusack, 1988; Angell, 1995) that provide a basis for the present discussion. The point of view often taken in analyses of ion beam amorphization (e.g., Averback and de la Rubia, 1998, and references therein) stresses the progressive build-up of disorder on a microscopic scale, i.e., the nature and stability of ion-induced damage, the consequences of defect cascade overlap, etc. These important aspects obviously cannot be neglected, but in this paper I attempt to discuss the crystal-to-glass transformation in terms similar to the classical discussion of the liquid-to-glass transition. Such a parallel has its pitfalls – the wealth of data existing on the latter has no equivalent for the former, and suggestive analogies are not proof – but it may suggest new directions for ion beam experiments and simulations.

I summarily recall a few general properties of glasses and of the liquid-to-glass transition, and point out results on ion beam-amorphized systems that may be analyzed in the same perspective, as regards static and dynamic properties. The results suggest the possibility that the ion-induced crystal-to-glass transformation may be analyzed in terms of a percolation transition similar to that proposed by Cohen and Grest (Cohen and Grest, 1979; Grest and Cohen, 1981) for the liquid-to-glass transition. Finally, a most remarkable feature of glass evolution is its relation to ergodicity: the final Section briefly discusses the possible influence of ion irradiation on this basic property. This paper is rather speculative – my excuse is the organizers' request to peer into the highly disordered crystal ball of "open problems".

2. Glasses and the Liquid-to-Glass Transition

How to produce the amorphous, or glassy, state? Starting from the liquid state, slow cooling leads to crystallization via a first-order phase transition at a well-defined temperature T_m. In order to form a glass, the liquid must be supercooled to a temperature below T_g, far below the melting temperature T_m (Figure 1a), at sufficient speed to avoid nucleation of stable crystallites. An amorphous system is thus intrinsically thermodynamically unstable, produced by the slowing-down of relaxation processes that would otherwise return it to the liquid (at high temperature) or some ordered crystalline structure (at low temperature). On a microscopic scale, these processes involve temperature-dependent atomic movements, lattice relaxation and lattice vibrations, which in turn depend on the bonding characteristics of the system (usually ionic for insulating glasses, covalent for amorphous semiconductors, and involving hybridized conduction electrons for amorphous metals). On the macroscopic scale, relaxation processes appear via the temperature evolution of the supercooled liquid's shear viscosity. As the liquid is cooled at a sufficiently fast rate, its viscosity increases; its volume and change of enthalpy decrease until – at a temperature termed the "glass temperature" T_g – both quantities deviate markedly from the extrapolated high-temperature curve, the deviation increasing as the temperature decreases. Just above T_g, the viscosity $\eta(T)$ changes dramatically (typically over more than ten orders of magnitude when the temperature is halved) according to the empirical so-called Fulcher–Vogel law (Cusack, 1988),

$$\eta(T) = \eta(0)\, \mathrm{e}^{A/[k_B(T-T_0)]}, \tag{1}$$

where T_0 is the temperature at which the viscosity diverges – the "free volume" in the glass vanishes. At T_g the viscosity is so high (typically above 10^{13} P) that the material no longer flows: if the liquid is kept at some temperature below – but fairly close to – T_g, the relaxation processes will continue (albeit extremely slowly), and carry the system from the "glass" curve to the extrapolated "supercooled liquid" curve. The crucial point is that the properties of a glass depend on its history, i.e., the initial state (temperature of the melt), cooling rate and quench temperature. As a result, T_g for a given substance is *non-unique* (Figure 1b), as opposed to the melting or freezing temperatures. The glass transition first appears as a kinetic transformation leading to configurational freezing, rather than as a thermodynamic phase transition (there is, in fact, a thermodynamic limitation that we ignore here – see the discussion of the "Kauzmann paradox" by Jäckle, 1986). The relaxation processes involved are sufficiently complex that when a given material becomes glassy, the final structural configuration on any scale is

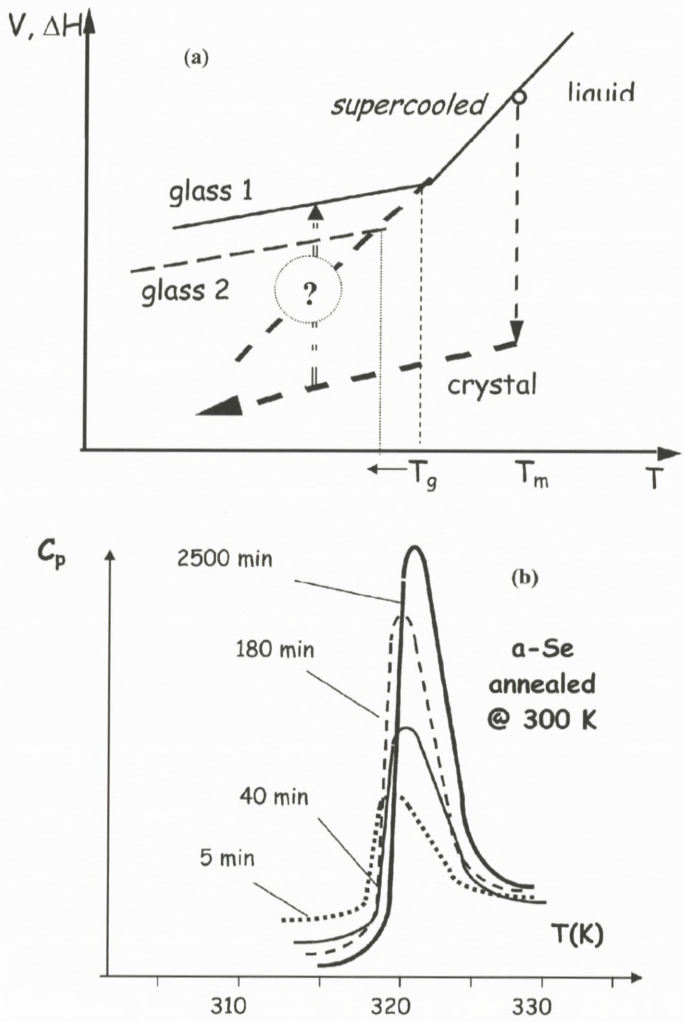

Figure 1. (a) Liquid-to-glass (*versus* liquid-to-crystal) transition as detected from volume or enthalpy change. The glass transition temperature T_g and the glass structure both depend on the cooling speed, leading to different glasses: glass 1, glass 2). The main point of this paper concerns the validity and consequences of the crystal-to-glass transition, denoted by the vertical arrow. (b) The specific heat displays a peak near the glass transition, but this is not a classical second-order phase transition. All curves were obtained after quenching from the same melt temperature, at the same speed and to the same final temperature T_f, well below T_g. After relaxing at T_f for varying times (shown in the figure), samples were annealed at constant speed: the height and position of the specific heat peak both depend on the system's relaxation towards its equilibrium configuration at T_f. Kinetics thus dominate the transition. Adapted from R.B. Stephens, J. Non-Crystalline Solids **20**, 75 (1976).

non-unique. Both the observed glass viscosity change and T_g therefore depend strongly on the ratio of the experimental measuring time to the average structural relaxation time. This also accounts for the specific heat variation shown in Figure 1b, since atomic motion is hindered below T_g, eliminating the relaxation contribution to the free energy. This prevents the viscous liquid from exploring the entire phase space (i.e., all atomic configurations): the system becomes non-ergodic. Glass relaxation, through diffusion or inverse viscosity, then takes place – the system only travels through a part of phase space that depends on the initial and quench conditions, i.e., the glass's past history. Such dynamics are a universal feature of glassy systems (polymers, oxides, metglasses, spin glasses, etc.) and remain a major challenge to theory. We shall return to this in the last section. The "time-window" effect is very relevant to a discussion of ion beam effects, since flux-dependent irradiation-induced (or -enhanced, if thermal effects are present) atomic displacements are the source of structural relaxation in irradiation experiments. The influence of atomic displacements also depends on the size of the structural unit involved in the relaxation process – the microscopic features of defects and defect motion mechanisms in a glass are a continuing subject of debate. In apparent contradiction with the abovementioned dynamics, a wealth of experiments (e.g., Perepezko, 2004) has established that structural stability criteria always play a major role in determining such static properties of glasses as the glass-forming composition range, the chemical short-range order (CSRO) distribution, the relative stabilities, etc., which are practically the same for nominally identical glasses prepared under such very different conditions as melt-cooling, quench-condensation on a cold substrate, solid-state reactions, ion implantation or ion beam mixing. This is a strong indication that the statics of amorphous phases may be related to free energy considerations and thermodynamic phase diagrams. How to reconcile these two aspects?

"Amorphous" does not mean random. On a near-neighbor scale (typically up to 3–5 atomic distances), the atomic arrangement in any amorphous system as determined by the atomic bonds shows that the interatomic distances and bonding angles for a given system display distributions as intuitively expected, but around well-defined average values that are those of some crystalline phase. Short-range order, or more precisely *chemical* short-range order (CSRO), can be defined for an amorphous system in the absence of long-range order. Rather narrow distributions in the number of atoms in a ring and among the bond angles on a short-range scale suffice to produce a solid with no long-range order, as evidenced in X-ray and neutron diffraction experiments, as well as extended X-ray atomic fine structure (EXAFS) experiments performed on all types of glasses. Whatever the nature of the chemical bond, such experiments and corresponding simulations

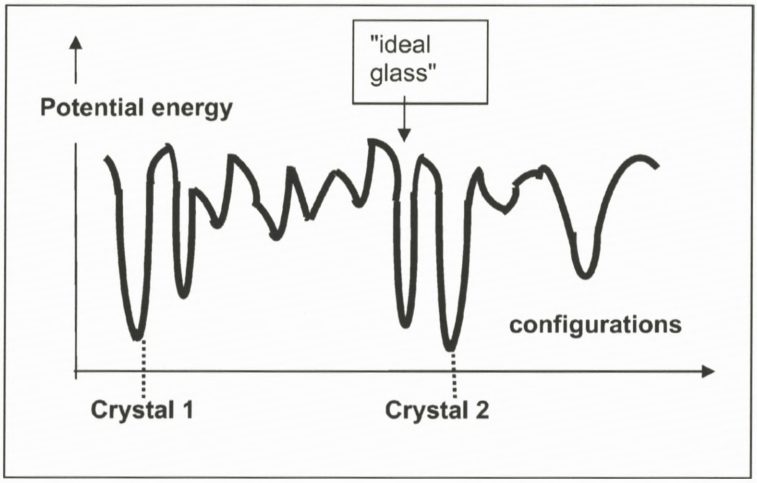

Figure 2. Schematic of potential energy curves corresponding to different possible configurations (i.e., different amorphous phases) of a glass, including the most stable (long-term annealed) glass. Two crystalline phases are also shown. The different configurations are traditionally accessed by different cooling rates. A transition from one configuration to some other is possible via, e.g., annealing or applied pressure, as shown by differential calorimetry, X-ray diffraction or EXAFS experiments.

always confirm the existence of a well- defined CSRO. On the other hand, the existence of *distributions* in the number of neighbors and interatomic distances shows that the free energy of a glass structure is not unique, as opposed to the case of a crystalline structure at the same composition, in which bond lengths and angles are single-valued. The existence and influence of medium-range order, typically beyond the third or fourth nearest neighbor seen in neutron diffraction or EXAFS, is also increasingly recognized and increases the number of possible structural configurations. There are thus (e.g., Laaziri et al., 1999; Sheng et al., 2006) a multiplicity of different amorphous states, corresponding to different minima in configurational space (Figure 2). The effect of irradiation on the short- and medium-range order scale in glasses is likely crucial to ion beam amorphization dynamics, as discussed below.

An analysis of the liquid-to-glass transition was provided by the free-volume theory of Cohen and Grest (1979) and Cohen and Grest (1981). The theory associates a volume v (initially the Voronoi polyhedron) with each molecule (or atom) in a liquid, and when atomic motion leads to v being larger than a critical value v_c, regards the excess volume as free; no local free energy is required for redistribution of free volume v_f among the molecules, and v_f is a fluctuating quantity

(related to fluctuations of the total free volume in the liquid); finally, transport only occurs when a molecule (or atom) acquires enough free volume. Thus the reduction, upon cooling, of molecular (or atomic) mobility – and of structural relaxation – is directly related to the free volume decrease and provides a path to Equation (1). A most important feature is that the above assumptions define two radically different types of cells, "solid-like" ($v < v_c$) and "liquid-like" ($v > v_c$), with free volume exchange only being performed among the latter under conditions (connectivity and a sufficient number of identical neighbouring cells) that are identical to those existing in high-density percolation, favoring dense, well-connected clusters over isolated sites. Denoting $p(T)$ the temperature-dependent fraction of liquid-like cells and p_c the high-density percolation threshold, the glass transition occurs at $p(T) = p_c$, i.e., when $p < p_c$, the system is a solid glass with non-connected finite liquid-like clusters; when $p > p_c$, an infinite liquid-like cluster allows molecular (or atomic) transport throughout the sample. The Cohen-Grest theory relates to thermodynamics by weighting the local free energy functions over the elementary cluster volume size distribution, and introducing an entropy term due to diffusive motion inside the liquid-like clusters.

The following discussion of the crystal-to-glass transition (Section 3) is based on the percolation analysis and on a reinterpretation of the "liquid-like" clusters in terms, not of viscosity or diffusivity, but of "shear transformation" (Falk and Langer, 1998) or "jamming" (Cates et al., 1998) zones. These zones appear in dynamical theories of shear deformation in amorphous solids, colloids or granular material as small (nanometer size) volumes that either block or allow inelastic rearrangements under shear stress, depending on their internal configuration relative to an applied shear stress orientation. Liu and Nagel (1998), Silbert et al. (2002) and Shi and Falk (2005) showed that such strain localization may also occur in the liquid-to-glass transition. In all cases, as the temperature is reduced the system, which at high temperature explored all possible configurations, progressively finds itself limited to the exploration of an increasingly small fraction of phase space – it becomes non-ergodic.

3. Mechanisms of Ion-Induced Amorphization

A thermodynamic crystal-to-glass transition is clearly energetically unfavourable (Figure 1): the transformation only occurs via the forcing due to the ion energy deposition. Irradiation-induced atomic displacements affect not only the phase stability but also the phase transformations, depending both on the temperature at which they occur and on the ion flux. For a discussion of how the combination of both parameters controls ("forces") atomic mobility, see Martin and Bellon

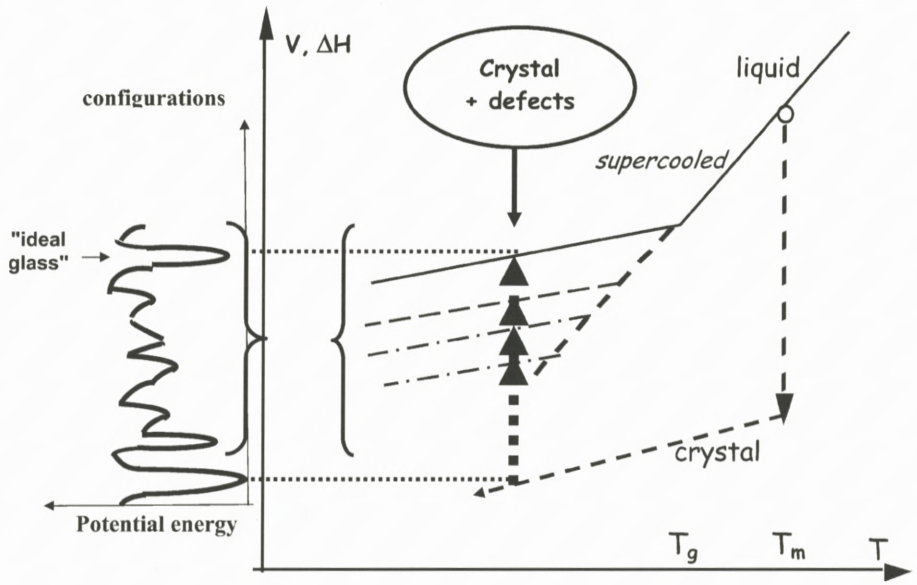

Figure 3. Relating Figure 1a to Figure 2. Different amorphous states (with different CSRO configurations) have different free energies: thermal annealing promotes relaxation from one of these states to a more stable one, while irradiation can allow (full arrows) the system to explore a variety of configurations, independently of their relative stability.

(1997). In this section, the emphasis is on those aspects of ion beam-induced amorphization of diverse materials from which a consistent view of the crystal-to-glass transition may be built. The detailed mechanisms clearly differ according to the nature of the chemical bonds in the irradiated materials, since the latter determine not only the short-range order (Section 1), but also the atomic mobility and the nature of defects.

3.1. Ion Beam Amorphization of Semiconductors

Because of their applications, a wealth of studies exists on semiconductors, and particularly on Si. As regards static properties, the most notable fact is the demonstration (e.g., Laaziri et al., 1999; Glover et al., 2001) via X-ray, neutron, EXAFS, Raman, differential calorimetry, and other experiments that there exist different amorphous states corresponding to different short-range order configurations, that these are accessible by irradiation, and that thermal annealing can promote relaxation from one of these states to a more stable one. This situation is schematized in Figure 3. The results are less clear-cut as regards the dynamical properties. In semiconductors, the dominating directional covalent bonds com-

plicate the amorphization process. The beam-induced crystalline-to-amorphous (c/a) transformation of elemental Si was first observed decades ago. A room-temperature amorphization curve under Si ion irradiation, may be determined via a precise Rutherford Backscattering (RBS) channeling experiment (e.g., Holland and Pennycook, 1989). The observed "damaged fraction" is actually the amorphous fraction α, as verified by transmission electron microscopy (TEM). The experimental curve may be fitted by

$$\alpha(\mathrm{c/a}) = 1 - \mathrm{e}^{-\sigma\phi}, \tag{2}$$

where ϕ is the ion fluence and σ a "damage cross-section" to be determined. Essentially identical curves (with different values of σ, ϕ) are obtained for different irradiating ions in different semiconducting materials. Of course, such a Poisson-type probability distribution does not provide a microscopic description of any specific mechanism. Does amorphization occur inside individual cascades (Morehead and Crowder, 1970), whose ultimate superposition would lead to overall amorphization in the implanted volume? Or is the driving force for transformation the storing of lattice defects, which locally raise the free energy of the sample above that of amorphous Si (Vook and Stein, 1969; Swanson et al., 1971)? The latter was favoured: if defects were only created in the cascade core, amorphization would be far less efficient than experimentally found, and many experiments showed that amorphization became more difficult or impossible just as defects became mobile. In fact, room temperature *in-situ* transmission electron microscopy (TEM) with an ion beam impacting the sample inside the TEM chamber (Ruault et al., 1983) clearly showed (Figure 4) that (for large deposited energy densities at least) both processes coexist, and there is actually a form of nucleation and growth in the amorphization process, mediated by the existence of defected zones outside of the cascade core. Thus, for elemental Si with covalent bonds, the transformation to the amorphous phase is neither unique nor a simple one. Both heterogeneous amorphization and, more frequently, a form of "local" homogeneous nucleation and growth occur in ion-irradiated samples. This rather agrees with the conclusions of Holland and Pennycook (1989). Specifically, the *in-situ* TEM experiments show that many strained-induced contrasts due to dislocations formed in the cascade core survive as amorphization proceeds, so that relatively long-range strain effects – also indicated in early MD simulations (Averback and de la Rubia, 1998) – contribute to lattice destabilization and subsequent amorphization. This feature will reappear when discussing evidence for "jamming" effects. Recent MD simulations (e.g., Pelaz et al., 2004; Lewis and Nieminen, 1996) detailed such structures, and concur with high resolution TEM experiments (Yamasaki 2002) showing that these defects resemble "amorphous nuclei" composed of 5- and 7-member Si rings.

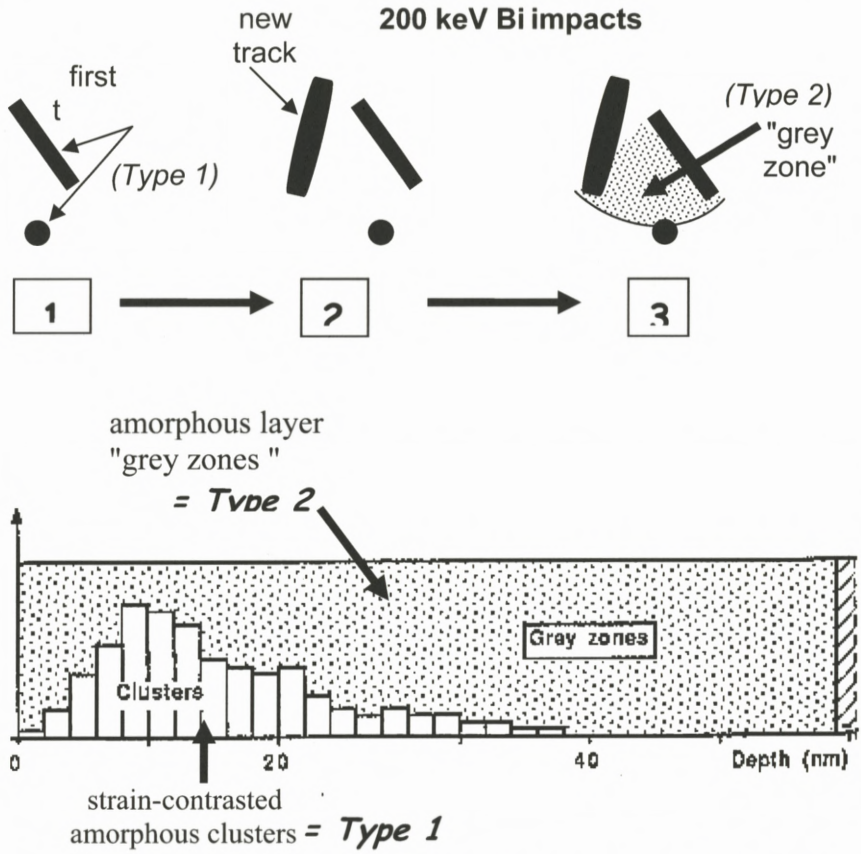

Figure 4. In-situ TEM experiment showing 200 keV Bi^+ ion-induced amorphization process in Si at 300 K. Upper: (1) Two impacts within ca. 60 nm have produced two high-contrast defected areas (dislocations: Type 1 damage); (2) a new impact occurs within ~60 nm, producing another Type 1-contrast area; (3) simultaneously, the entire area within the three impact tracks becomes "grey", identified by selected area diffraction as amorphous (Type 2 damage). Lower: comparing the defect cluster depth histogram as measured via TEM with the amorphous layer thickness as measured by RBS/channeling. The amorphous area extends well beyond the dislocation (Type 1 damage) distribution. Type 1 damage anneals at 500 K; Type 2 damage anneals at 800 K. Figure from Ruault et al. (1983).

3.2. Combining Kinetics and Chemistry: Amorphization of Metallic Alloys

The analysis of crystalline-to-amorphous transformations in metallic alloys containing two or more components with attractive potentials is very informative

because it relates more directly to equilibrium phase diagrams. A simple ordered intermetallic compound (e.g., ABABABA... sequences along one or more low-index directions) may be affected by irradiation via chemical disordering or structural defect accumulation (individual replacements or replacement sequences). The initial crystal lattice structure is preserved if the ordering energy is lower than the energy difference between the amorphous and crystalline states (irradiation-induced ordering may actually occur in this way, see Bernas et al., 2003); the reverse case can lead to amorphization. Experiments and MD simulations indicate that chemical disorder may suffice to amorphize (Massobrio et al., 1990), whereas in other instances (e.g., Sabochik and Nghi, 1990) chemical disordering occurs first, with subsequent amorphization due to defect accumulation in the destabilized lattice. The relative free energies, the initial and final states' stability, interfacial energies and strain all play a role, which we ignore here in searching for general features. We stress, rather, that the progressive amorphization of the $NiZr_2$ system and the correlated change in elastic properties was very well described (Massobrio et al., 1990) by high-density bond percolation of the chemically disordered zones. Crucial information also comes from the amorphizing system's dynamics, since its evolution is driven by a continuous flow of atomic displacements producing first antisite defects, then local order restructuring. Essential results (Watanabe et al., 2003) in this area are discussed in Section 4.

3.3. The Case of Metal-Metalloid Compounds

The transition metal-metalloid compounds around the deep eutectic composition (e.g., Fe_3B, $Ni_{80}P_{20}$, $Pd_{80}Si_{20}$, ...) were the first "metglasses" produced by ultraquenching, due to the presence of covalent metalloid bonds and to the corresponding structural complexity of many of their ordered phases. Starting from the crystalline variety of these compounds, irradiation-induced amorphization occurred at low fluences, in the 0.1 dpa (displacements per atom) range, and the amorphization fluence dependence resembled that of Equation (2).

Alloys of the same nominal composition may be produced by direct implantation of the metalloid into the initially pure crystalline metal, thus providing information on the amorphization dynamics. For example, a combined channeling and *in-situ* TEM study (Cohen et al., 1985; Schack, 1984) of progressive amorphization of P-implanted Ni as a function of the implantation-induced compositional change showed (Figure 5) that at 80 K (precluding defect or atom movement) the amorphous fraction α varies as

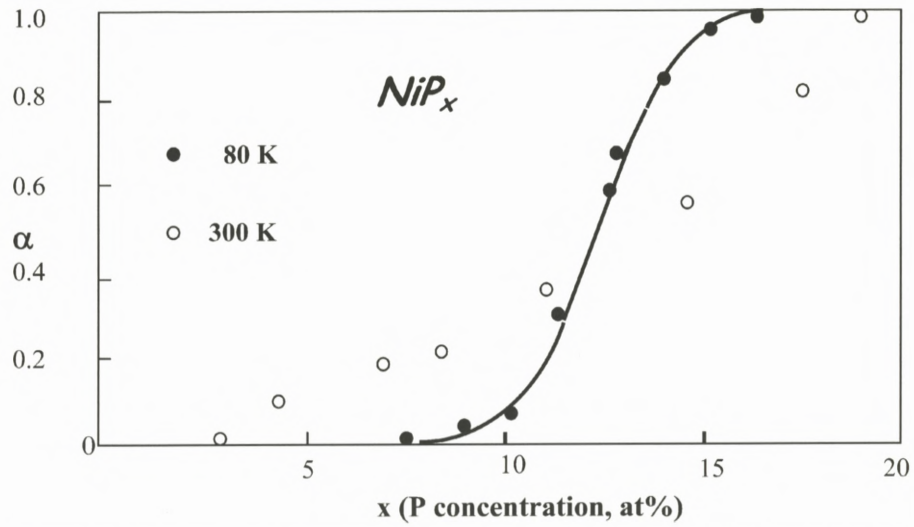

Figure 5. Dependence of amorphous fraction α on concentration x of 100 keV P ions implanted into Ni at 80 K or 300 K. Solid line: best fit to 80 K results with Equation (3) and a critical volume v_c of radius ~1 nm. At 300 K, both collisional defects and P atoms move under implantation; amorphous clusters grow, so that the percolation model is no longer appropriate. Adapted from Cohen et al. (1986).

$$\alpha = \sum_{N=N_C}^{\infty} \frac{(\bar{N})^N}{N!} e^{-\bar{N}}, \tag{3}$$

where it is assumed that amorphization proceeds by a build-up of implantation-induced elementary amorphous clusters of volume v_c, synthesized when $N \geq N_C$, whose size is obtained from a single-parameter fit to Equation (3). The average number $\bar{N}$ of P atoms in a cluster is proportional to the latter's volume and to the mean P concentration c_c in the sample. The "amorphization threshold" corresponds to a critical concentration of $c_c = 12\%$ at 80 K. At these implant concentrations, defect density saturation has long been reached, so amorphization is essentially due to chemical effects, just as it was due to chemical disordering when irradiating intermetallic alloys such as NiTi or the metal-metalloid compounds at the deep eutectic composition.

The radius of the critical volume v_c is found to correspond to the distance over which the CSRO may be defined according to EXAFS, X-ray or neutron diffraction measurements. The same features were found in many similar amorphization experiments, the elementary cluster size remaining the same and the critical concentration depending on the initial lattice structure. The size deduced

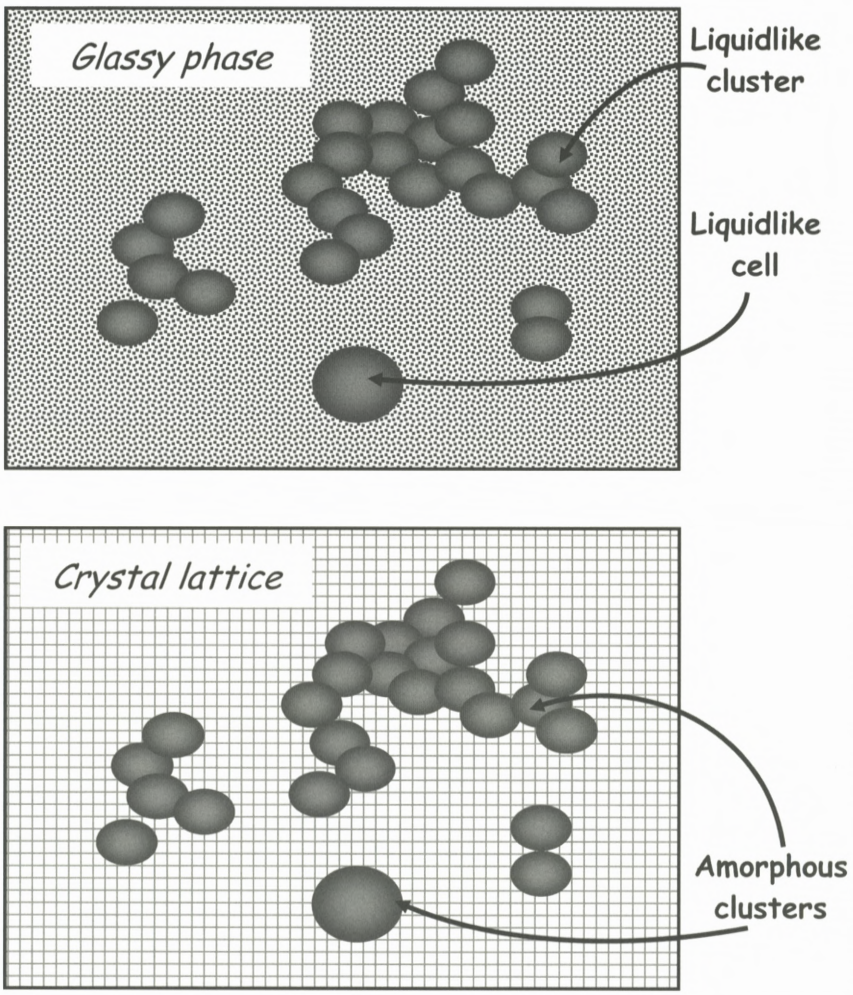

Figure 6. Schematic view of the proposed ion beam-induced amorphization mechanism (lower part), compared to a schematic of the free-volume theory of Cohen and Grest (upper part). Percolation of transformed zones plays the major role in each case.

from the fit to Equation (3) is an indication that, at least for those metglasses whose CSRO is determined by covalent bonds, the amorphous lattice results from a progressive accumulation of nanometer-size elements, whose packing properties are presumably determined both by the CSRO around a solute atom and by the organization of the initially crystalline host. This geometrical aspect suggests the following percolation description.

4. The Nature of the Amorphization Threshold: A Crystal-to-Glass Transition?

The ultimate purpose of this section will be to examine possibly common features of the liquid-to-glass and crystal-to-glass transition, and their differences. First, consider the static properties. As noted above, the "free volume" theory, based on the notion that glasses contain extra volume relative to the crystalline phase with atomic transport being possible only between the corresponding "open cells", projects the glass transition problem onto that of a percolation transition. Percolation theory only requires that the physical structure of the "open cells" be defined by geometry (i.e., whether connections between "lattice points" are determined by sites or by bonds). As a first step, analyzing amorphous materials properties in this way can provide a guide for comparison with MD simulations based on different assumptions regarding the elementary entities that form a glass. Can the implantation-induced amorphization process in NiP_x be analyzed by a percolation model? In writing Equation (3), it was assumed that the initial fcc Ni lattice was progressively filled (Figure 6) by elementary nm-size amorphous volumes. As the concentration of these building-blocks increases, they randomly connect to each other in the fcc lattice and the observed amorphization threshold at 12% is just the three-dimensional bond-percolation threshold of the fcc lattice. (At higher temperatures, the combination of irradiation and thermal activation leads to time fluctuations, diffusion and growth – static percolation no longers holds.) A recent detailed experimental, simulation and modeling study of atomic arrangements in both metal-metal and metalloid-metal (including Ni-P) metglasses (Sheng et al., 2006) has shown that at comparatively low concentrations, solute atoms surround themselves with near-neighbor solvent atoms only, forming different types of icosahedra-like clusters which in turn tend to form "clusters of clusters" via symmetry and connectivity rules. The ion beam amorphization process suggested above is entirely consistent with this picture.

Now consider the dynamic, notably viscoelastic, properties which are a major feature of glasses (Anderson, 1979). Here, we are confronted with the special case of a heterogeneous system, with both a crystalline and an amorphous component. In the case of intermetallics the onset of amorphization is experimentally found to be accompanied (Grimsditch et al., 1987) by a drastic softening of the elastic properties. MD simulations (Massobrio et al., 1990) showed that this effect is directly related to the production of "distorted volumes" by accumulation of antisite defects, and that these volumes percolate with a threshold concentration of 15% (the material is bct), leading to an abrupt increase in the shear modulus. Metal-metalloid systems such as NiP_x or $PdSi_x$ which include both metallic

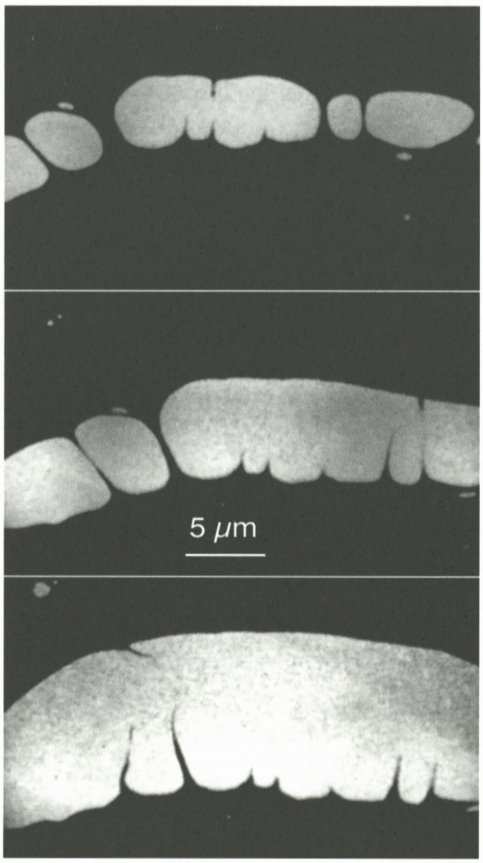

Figure 7. In-situ TEM observation of shear thinning, shear tearing and viscoplastic flow during Si ion implantation into Pd. The figure shows three stages of the same sample area (about 20% increase of the Si concentration between upper and lowest frame) just above the percolation threshold of the amorphous volumes (Schack, 1984).

and covalent bonds are expected to form even more highly distorted volumes leading to larger localized strain, inducing shearing at and above the percolation threshold. This is indeed shown (Figure 7) by *in-situ* TEM experiments (Schack, 1984) on unsupported films. As the implanted metalloid concentration increases in the metal, periodic stress appears in the film (not shown in the figure). When the metalloid concentration reaches the percolation threshold, shear thinning and shear softening abruptly lead to viscous flow and subsequent tearing of the film. The consequences of stress in fully amorphous materials are accounted for (Shi and Falk, 2005; Silbert et al., 2002) by MD simulations assuming the existence of

small volumes (estimated size typically on the nm, CSRO scale) in which stress is localized ("jammed"). Percolation of these "shear transformation zones" corresponds to a threshold for plastic flow, leading to progressive "unjamming" by the creation and disappearance of such trapping volumes. In quenched glasses, the "unjamming" is provided by the strain-rate induced deformation (i.e., changing the quenching speed). My interpretation of the heterogeneous system's behavior in Figure 7 is that the nanometer-sized amorphous volumes inside the residual crystal are also shear transformation zones, the difference being that they are inactive below the percolation threshold. The specific feature of ion beam experiments is that viscous flow sets in quite *suddenly* as soon as the percolation threshold is met. This is ascribed to the constant creation and destruction of "jamming volumes" by successive collisional displacements that accompany metalloid implantation. Above the percolation threshold, even negligible changes in the metalloid concentration correspond to intense structural reorganization via atomic motion on the nm scale. As noted previously, this can correspond to transformations of CSRO among the available local quasicrystalline structures that stabilize the glass configuration (Shi and Falk, 2005), and many tens of such structures have been found (Sheng et al., 2006).

The above picture of the ion-induced crystal-to-glass transition relates it to the liquid-to-glass transition, insofar as the active entities have the same (nanometer) size and the same basic role (shear transformation zones) in both cases. The picture is consistent with available information on the possible variations of CSRO, allowing structural modifications of the shear transformation zones; it is also consistent with the small size scales (due to low energy recoils) and induced stress of defected zones found by MD simulations in ion cascades (Averback and de la Rubia, 1998; Nordlund, 2006). A very interesting indication in the same direction was obtained in a series of *in-situ* high resolution TEM studies (Watanabe et al., 2003) performed during NiTi amorphization (requiring both chemical and defect-induced contributions) by high-energy electron irradiation. These experiments studied the local (nanometer scale) structure under irradiation and found that, while the average number of nanometer-size amorphous zones increased continuously as irradiation proceeded, the amorphous zone formation process was actually *discontinuous and even reversible*: due to atomic displacements, ion flux- and fluence-dependent structural fluctuations occurred under irradiation between the ordered and amorphous phases for a given observed zone. Thus, under irradiation and for this size scale, the free energy difference between one of the possible glass states and some metastable unrelaxed defect state is presumably small and easily modified by the irradiation. Moreover, their power spectrum reveals that the temporal fluctuations of the local order parameter are correlated. These results

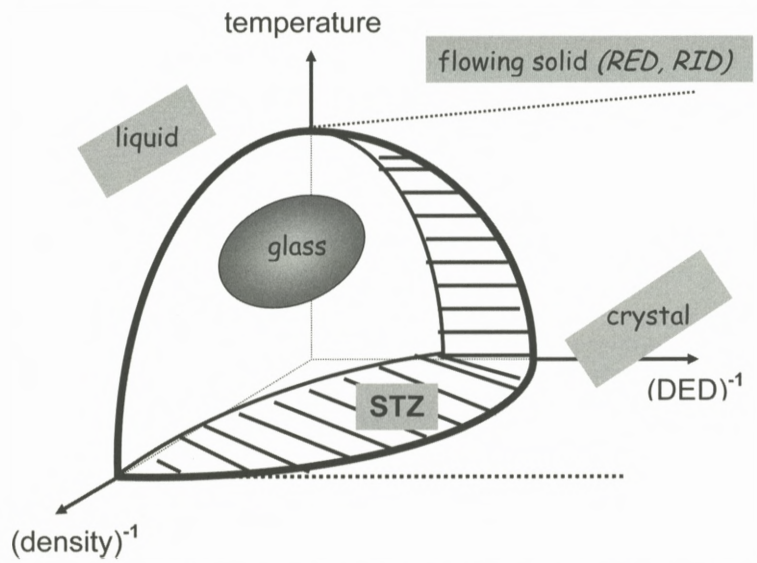

Figure 8. Proposed phase diagram relating both the liquid-to-glass and the (irradiation-induced) crystal-to-glass phase transitions to jamming. Both transitions are assumed to be driven by the formation of shear transformation zones (STZ – hatched volume). The axes are the temperature, the inverse density and the inverse deposited energy density (DED). The outer surface marks the frontier between ergodic and non-ergodic processes. (RED stands for radiation-enhanced diffusion; RID for radiation-induced diffusion).

detail the time-dependence of amorphization, and add confidence to the picture presented above.

We saw that as a system approaches the liquid-to-glass transition (just as for the jamming transition in granular or colloidal materials), it finds itself progressively restricted in its exploration of phase space. If we consider the NiP_x ($PdSi_x$) or NiTi systems as a whole, their evolution under ion-induced amorphization is towards non-ergodicity, and increasingly so as they become totally amorphous. From all the information gathered above, a tentative phase diagram may be drawn where the variables are the temperature, the density and the deposited particle energy density (Figure 8). This figure was suggested by the phase diagram proposed by Liu and Nagel (1998), relating the liquid-to-glass transition to dynamic jamming in granular materials. It is extended to a relation between dynamic jamming and *both* the liquid-to-glass and crystal-to-glass transitions. The drawn outer surface separates ergodic from non-ergodic processes; the hatched volume corresponds to the jamming processes or, more exactly, to the processes where shear transformation zones are active in the crystal-to-glass transition. The diagram suggests

that ion irradiation experiments could be a very adequate means to explore novel aspects of the crystal-to-glass transition, as well as a new tool to explore the liquid-to-glass transition.

5. Ion Beams to Study Glasses?

Consider – in the same samples as above – the subsystem constituted by (i) the nm-sized amorphous clusters inside the crystalline lattice and (ii) for the implanted NiP_x alloy, a time-window and a beam flux such that the displaced atom rate is high, but with no significant concentration change. Because of collision-induced restructuring of the small entities, the evolution of this subsystem is no longer restricted to a limited region of phase space: although the macroscopic system is non-ergodic, *for the nm-scale entities, the evolution tends to become ergodic*, even to the point (Watanabe et al., 2003) where some amorphous clusters revert to the crystalline state while others are subject to the reverse transformation. When the amorphous clusters pervade the whole sample and render it "uniformly amorphous" (thus a non-ergodic metglass), we may still divide up the metglass into nm-sized volumes as before, since this is the scale over which irradiation modifies the local structure and determines the evolution of the jamming site population. If the displacement rate is large enough, the evolution of this sub-population is essentially ergodic under irradiation, and this can affect the overall viscoelastic properties of the glass. The existence in physical systems of components with differing ergodicities (Palmer, 1982) is not exceptional (e.g., in magnetism). But particle irradiation is a physical tool that modifies the statistical, as well as the structural, behavior of the overall system's crucial (CSRO-scale) component. By subjecting a non-ergodic glass to an appropriate combination of ion-induced and thermal atomic mobility, its nanoscale subsystem may become ergodic and might even explore the crystalline phase; this way of looking at the sometimes-observed irradiation- induced amorphous-to-crystalline transformation is akin to a "driven alloy" analysis (Martin and Bellon, 1997).

Another, perhaps even more intriguing possible area for research is that of glasses *per se*, and of the liquid-to-glass transition. To my knowledge, there has been no ion beam work in this field, so the following remarks are speculative. As noted in Section 1, understanding why the dynamic evolution of glass non-equilibrium properties have universal features, as well as the origin of the latter, is a major long-standing problem in condensed matter physics. This is related to the crucial property of "aging" (Cipelletti and Ramos, 2005; Vincent et al., 1997), i.e., the continuous time evolution with sample age (e.g., time elapsed since glass quench) of such characteristic properties as the viscosity, strain relax-

ation, or magnetization in spin glasses. Aging most often involves both reversible quasi-equilibrium "fast" fluctuations and irreversible changes that are increasingly slow as the sample ages. What are the relations between the "slow" and "fast" processes (Sibani and Jensen, 2005; Mazoyer et al., 2006)? Can the corresponding dynamic correlation functions be experimentally identified (Berthier et al., 2005), and possibly acted on? Studies of these processes focus on the temperature range around T_g, largely because there is a reasonable experimental time window (relaxation phenomena are on the 100-second scale when the viscosity is around 10^{13} poise). Irradiation experiments could open new vistas. Under irradiation at low temperature the nanoscale dynamics become ergodic, directly controlled by statistical collisions due to the particle beam rather than to the temperature – the "observational time window" (which is actually an average collision time in a nm-size volume of the sample) depends on the beam intensity, which is also a control parameter of the ergodicity. This opens the possibility of examining directly whether and how acting on the nanoscale configuration and dynamic correlation length affects the slow dynamics' evolution. The results of Figure 7 suggest a significant influence indeed, but of course this requires confirmation in a "homogeneous" glass. More generally, irradiation experiments should also explore conditions where the temperature plays a more significant role, in the range nearer to (but still far below) T_g where thermal relaxation times are considerably shorter and so comparison and overlap with existing glass studies and models can be made.

Acknowledgements

It is a pleasure to acknowledge Peter Sigmund for many thought-provoking discussions during our collaborations and encounters over the years. I am also grateful to the participants of ION'06 for fruitful debate on several problems related (or not) to the topic of this paper. This work owes a major debt to my colleagues at CSNSM – Orsay, especially M.-O. Ruault, and was initially stimulated by an argument with P. Averbuch. I wish to thank S. Lipinska for the gracious hospitality of Moulin d'Andé.

References

Anderson P.W. (1979): Lectures on amorphous systems. In: Balian R., Maynard R. and Toulouse G. (Eds), Ill-Condensed Matter. North Holland, Amsterdam, pp 159–258

Angell C.A. (1995): Formation of glasses from liquids and biopolymers. Science **267**, 1924–1935

Averback R.S. and de la Rubia T.D. (1998): Displacement damage in metals and semiconductors. Solid State Phys. **51**, 281

Bernas H., Attane J.P., Heinig K.H., Halley D., Ravelosona D., Marty A., Auric P., Chappert C. and Samson Y. (2003): Ordering intermetallic alloys by ion irradiation: A way to tailor magnetic media. Phys Rev Lett **91**, 077203

Berthier L., Biroli G., Bouchaud J.P., Cipelletti L., El Masri D., L'Hote D., Ladieu F. and Perino M. (2005): Direct experimental evidence of a growing length scale accompanying the glass transition. Science **310**, 1797–1800

Cates M.E., Wittmer J.P., Bouchaud J.P. and Claudin P. (1998): Jamming, force chains, and fragile matter. Phys Rev Lett **81**, 1841–1844

Cipelletti L. and Ramos L. (2005): Slow dynamics in glassy soft matter. J. Phys. Cond. Matter **17**, R253–R285

Cohen M.L. and Grest G.S. (1979): Liquid-glass transition, a free-volume approach. Phys. Rev. B **20**, 1077–1098

Cohen C., Benyagoub A., Bernas H., Chaumont J., Thome L., Berti M. and Drigo A.V. (1985): Transformation to amorphous state of metals by ion-implantation: P in ni. Phys Rev B **31**, 5–14

Cusack N.E. (1988): The Physics of Structurally Disordered Matter. Adam Hilger, Bristol

Falk M.L. and Langer J.S. (1998): Dynamics of viscoplastic deformation in amorphous solids. Phys Rev E **57**, 7192–7205

Gibbons J.F. (1972): Proc IEEE **60**, 1062

Glover C.J., Ridgway M.C., Yu K.M., Foran G.J., Desnica-Frankovic D., Clerc C., Hansen J.L. and Nylandsted-Larsen A. (2001): Structural-relaxation-induced bond length and bond angle changes in amorphized Ge. Phys Rev B **6307**, 073204

Grest G.S. and Cohen M.L. (1981): Liquids, glasses, and the glass transition: A free-volume approach. Adv Chem **48**, 455

Grimsditch M., Gray K.E., Bhadra R., Kampwirth R.T. and Rehn L.E. (1987): Brillouin-scattering study of lattice-stiffness changes due to ion irradiation – Dramatic softening in Nb_3Ir. Phys Rev B **35**, 883–885

Holland O.W. and Pennycook S.J. (1989): New model for damage accumulation in si during self-ion irradiation. Appl Phys Lett **55**, 2503–2505

Jäckle J. (1986): Models of the glass transition. Rep Progr Phys **49**, 171–231

Joffrin J. (1979): Disordered systems-experimental. In: Balian R., Maynard R. and Toulouse G. (Eds), Ill-Condensed Matter. North Holland, Amsterdam, pp 63–154

Landau L. and Lifshitz I.M. (1958): Statistical Physics, Addison-Wesley

Laaziri K., Kycia S., Roorda S., Chicoine H., Robertson J.L., Wang J. and Moss S.C. (1999): High resolution radial distribution function of pure amorphous silicon. Phys Rev Lett **82**, 3460–3463

Lewis L.J. and Nieminen R.M. (1996): Defect-induced nucleation and growth of amorphous silicon. Phys Rev B **54**, 1459–1462

Liu A.J. and Nagel S.R. (1998): Nonlinear dynamics – Jamming is not just cool any more. Nature **396**, 21–22

Martin G. and Bellon P. (1997): Driven alloys. Solid State Phys Adv Res Appl **50**, 189–331

Massobrio C., Pontikis V. and Martin G. (1990): Molecular-dynamics study of amorphization by introduction of chemical disorder in crystalline $NiZr_2$. Phys Rev B **41**, 10486–10497

Mazoyer S., Cipelletti L. and Ramos L. (2006): ArXiv preprint cond-mat/0603739

Morehead F.F. and Crowder B.L. (1970): A model for the formation of amorphous Si by ion bombardment. Rad Eff Def Sol **6**, 27–32

Nordlund K. (2006): Radiation damage in carbon nanotubes: What is the role of electronic effects? Mat Fys Medd Dan Vid Selsk **52**, 357–370

Palmer R.G. (1982): Broken ergodicity. Adv Phys **31**, 669–735

Pelaz L., Marques L.A., Aboy M. and Barbolla J. (2004): Atomistic modeling of ion beam induced amorphization in silicon. Nucl Instr Meth Phys Res B **216**, 41–45

Perepezko J.H. (2004): Nucleation-controlled reactions and metastable structures. Progr Mater Sci **49**, 263–284

Ruault M.O., Chaumont J. and Bernas H. (1983): Transmission electron microscopy study of ion implantation induced Si amorphization. Nucl Inst Meth **209–210**, 351–356

Sabochick M.J. and Nghi Q.L (1991): Radiation-induced amorphization of ordered intermetallic compounds CuTi, $CuTi_2$, and Cu_4Ti_3: A molecular-dynamics study. Phys Rev B **43**, 5243

Schack M. (1984): PhD Thesis, University of Paris XI

Sheng H.W., Luo W.K., Alamgir F.M., Bai J.M. and Ma E. (2006): Atomic packing and short-to-medium-range order in metallic glasses. Nature **439**, 419–425

Shi Y. and Falk M.L. (2005): Strain localization and percolation of stable structure in amorphous solids. Phys Rev Lett **95**, 095502

Sibani P. and Jensen H.J. (2005): Intermittency, aging and extremal fluctuations. Europhys Lett **69**, 563–569

Silbert L.E., Ertaş D., Grest G.S., Halsey T.C. and Levine D. (2002): Analogies between granular jamming and the liquid-glass transition. Phys Rev E **65**, 051307

Swanson M.L., et al. (1971): Radiat Eff **9**, 249

Vincent E., Hamman J., Ocio M., Bouchaud J.P. and Cugliandolo L.F. (1997): Slow Dynamics and Aging in Spin Glasses, Lecture Notes in Phys. Vol. 492. Springer Verlag, Berlin p 184

Vook F.L. and Stein, H.J. (1969): Radiat Eff **2**, 23

Watanabe S., Hoshino M., Koike T., Suda T., Ohnuki S., Takahashi H., Lam N.Q. (2003): Temporal fluctuation and its power law in the crystalline-to-glass transition during electron irradiation. Phil Mag **83**, 2599–2619

Zallen R. (1983): The Physics of Amorphous Solids. John Wiley, New York